Chemical Engineering Journal 149 (2009) 353–362

Contents lists available at ScienceDirect

Chemical Engineering Journal

journal homepage: www.elsevier.com/locate/cej

Modified mathematical model for gas phase olefin polymerization in fluidized-bed catalytic reactor

Ahmmed S. Ibrehem [a], Mohamed A. Hussain [a,*], Nayef M. Ghasem [b]

[a] Department of Chemical Engineering, University of Malaya, 50603 Kuala Lumpur, Malaysia
[b] Department of Chemical & Petroleum Engineering, UAE University, Al-Ain, P.O. Box 17555, UAE

ARTICLE INFO

Article history:
Received 8 January 2008
Received in revised form 13 May 2008
Accepted 13 May 2008

Keywords:
Fluidized-bed reactor
Olefin polymerization
Mathematical model
Dynamic studies

ABSTRACT

A modified model for the gas phase catalyzed olefin polymerization fluidized-bed reactors (FBR) using Ziegler–Natta catalyst is presented in this study. This mathematical model accounts for mass and heat transfer between the bubbles and the clouds without chemical reaction, between the clouds and the emulsion without chemical reaction, and between emulsion and solid with chemical reaction that occurs at the surface of the catalyst particles. The model accounts for the effect of catalyst particles type and porosity on the rate of reaction. In this work, the concentration and temperature profiles in the bubble, and emulsion phases are calculated and the effect of catalyst solid phase on the system is estimated. The effect of important reactor parameters such as superficial gas velocity, catalyst injection rate, and catalyst particle growth on the dynamic behavior of the FBR is investigated and the behavior of mathematical model is compared with the reported models for the *constant bubble size model*, *well-mixed model and bubble growth model* . Moreover, the results of the model are compared with the experimental data in terms of molecular weight distribution and polydispersity of the produced polymer at steady state. A good agreement is observed between our model prediction and the actual plant data.

1. Introduction

The general classification of polyethylene semi-batch reactor models has been considered by many previous studies. Generally, three main models exist namely; *constant bubble size model* [1], *well-mixed model* [2] *and bubble growth model* [3].

These reactor models can be divided into homogeneous and heterogeneous categories. The *pseudo-homogeneous polyethylene* models are the simplest to use in catalyst bed batch reactor modeling. The basic assumption made is that the reactor can be described as an entity consisting only of a single (liquid or gas) phase. *On the other hand*, heterogeneous models are used mainly for the case of gas phase polyethylene semi-batch reactors. These use heterogeneous catalysis because of the multi-phase nature of the process (liquid–solid phase or gas–solid phase) and also involve inter-phase mass transfer, heat transfer and chemical reaction [4,5].

Heterogeneous models are used widely especially in polymerization system [5,6]. Current research in this important area can be divided into two parts namely; mathematical models for fixed bed catalyst reactor systems and mathematical models for fluidize bed catalytic reaction for production of polyethylene. Chatzidoukas et al. [4] where the improved heterogeneous model considers the distinction between the gas phase and solid phase. Varma (1981) included mixing in the axial direction. Sala et al. [5] developed a two dimensional mathematical model where concentration and temperature patterns in the reactor can be predicted. Zeman and Amundson [6], Zheng et al. [7], Zavala et al. [8] improved the dynamic optimization of a semi-batch reactor for polyurethane production, Hatzantonis et al. [3] further improved the two-phase model of the polymerization system. In previous works, mass transfer with chemical reaction in fluidized-bed systems either consider all phases (Kunii and Levenspiel, 1969) or the emulsion phase alone (Choi and Ray, 1985; McAuley et al., 1994) [3,7–9].

In this study the contribution in the modified modeling is by including the catalyst phase and considering all three phases as compared to the other models i.e., constant bubble size model, well-mixed model and the bubble growth model. Simulations were also performed to study the effect of superficial velocity and catalyst flow rate in the bubble and emulsion phases. Comparisons with actual plant data at steady state were also performed.

* Corresponding author. Fax: +603 79675319.
E-mail address: mohd_azlan@um.edu.my (M.A. Hussain).

1385-8947/$ – see front matter © 2008 Elsevier B.V. All rights reserved.
doi:10.1016/j.cej.2008.05.014

Nomenclature

Ar	Archimedes number $[= d_p^3 \rho_g(\rho_s - \rho_g)g/\mu^2]$
A_{sf}^k	fraction of metal that can form "k" catalyst active
A_B	cross sectional area of bubble phase (m^2)
A_1	cross-sectional area of the bed (cm^2)
C_d^k	concentration of deactivated catalyst active sites (mol/cm^3)
C_{pg}	specific heat capacity of gaseous stream (cal/g/K)
C_{PMi}	specific heat of "I" monomer (cal/mol/K)
$C_{p,pol}$	specific heat capacity of polymer product (cal/g/K)
$C_{A\cdot S}$	adsorbed surface concentration of A in kmol/kg catalyst
$C_{B\cdot S}$	product desorption of B in kmol/kg catalyst
C_B	product concentration (kmol/kg catalyst)
C_V	vacant molar concentration sites (kmol/kg catalyst)
C_{cat}	mass fraction of catalyst in the solid phase
C_{AB}	concentration of monomer gas in bubble phase (kg/m^3)
C_{Ac}	concentration of monomer gas in cloud phase (kg/m^3)
C_{Ae}	concentration of emulsion phase (kg/m^3)
d_{bm}	maximum stable bubble size (cm)
d_p	particle diameter (cm)
d_b	bubble diameter (cm)
D_g	gas self-diffusion coefficient (cm^2/s)
D_n^k	concentration of "dead" copolymer chains (mol/cm^3)
D_{bed}	bed diameter (m)
h	random bed height (m)
H	total bed height (cm)
H_{mf}	bed height at minimum fluidization conditions (m)
H_{bc}	bubble to cloud heat transfer coefficient ($cal/m^3/s/K$)
H_{ce}	cloud to emulsion heat transfer coefficient ($cal/m^3/s/K$)
H_{be}	bubble to emulsion heat transfer coefficient ($cal/m^3/s/K$)
$[H_2]$	hydrogen concentration (mol/m^3)
k_g	gas thermal conductivity (J/m/s/K)
k_i	rate constant of reaction (l/s)
k_A	thermal conductivity between layers of catalyst particles ($J/m^2/s/K$)
k^n	rate constant of spontaneous reaction (l/s)
k^f	rate constant of chain transfer (l/s)
K_{bc}	bubble to cloud mass transfer coefficient (l/s)
K_{ce}	cloud to emulsion mass transfer coefficient (l/s)
K_{be}	bubble to emulsion mass transfer coefficient (l/s)
K^h	rate constant of chain transfer to hydrogen (l/s)
MFI	melt flow index of polymer (g/10 min)
$[M_e]$	active metal concentration (mol Me/m^3)
$[M_i]$	"I" monomer concentration (mol Me/m^3)
P_A	partial pressure of A in gas phase
P^0	potential active sites ($kmol/m^3$)
P_0	active sites concentration ($kmol/m^3$)
PDI	polydispersity index
Q_0	volumetric product removal rate (m^3/s)
r	radius (m)
r_a	rate expression for the active sites (kmol/kg catalyst)
$R_{\mu n,i}^k$	rate expression for live moments
$R_{vn,i}^k$	rate expression for dead moments
R_X^k	reaction rate of species X at "k" catalyst activesites ($mol/m^3/s$)
S_P^k	concentration of potential "k" catalyst active sites (mol/m^3)
T	temperature (K)
T_b	temperature in the bubble phase (K)
T_{ref}	reference temperature (K)
T_e	emulsion phase temperature (K)
T_w	wall temperature (K)
T_{fs}	temperature of inlet catalyst (K)
T_f	temperature of the feed gas (K)
u_{mf}	minimum fluidization velocity (m/s)
u_e	emulsion gas velocity (m/s)
V	volume (m^3)
Z	bed height (m)

Greek letters

α	ratio between weak to bubble volume
δ_b	bubble phase volume fraction
δ^*	fraction of fluidized-bed consisting of bubbles
$\Delta H_{r\times n}$	heat of reaction (kJ/kg)
ε	void fraction of the bed at minimum fluidized velocity
μ_g	viscosity of gas (g/cm/s)
μ_0^k	live polymer zero
μ_1^k	live polymer
μ_2^k	live polymer
v_0^k	dead polymer
v_1^k	dead polymer
v_2^k	dead polymer
π	constant ratio
ρ_s	solid density (kg/m^3)

Subscripts/superscripts

B	bubble phase
cat	catalyst property
e	emulsion phase
k	type of catalyst active site
mf	minimum fluidization conditions
n	compartment number
ref	reference value
1	monomer gas ethylene
2	monomer gas butane

2. Description of the improved mathematical model

2.1. Fluidized-bed system

In the fluidized-bed system considered here as seen in Fig. 1, the reactant gas enters the bottom of the bed and flows up the reactor in the form of bubbles. As the bubbles rise, mass transfer of the reactant gases takes place between the bubbles and the clouds and between the clouds and the emulsion without chemical reaction. The mass transfer between emulsion and solid with chemical reaction happens on the surface of the catalyst particles.

The model accounts for the type of catalyst particles and catalyst porosity. This is due to their effects on the rate of reaction as shown in Fig. 1. The product then flows back into the bubble and finally exits when the bubble reaches the top of the bed. The rate at which the reactants and products transfer in and out of the bubble affects the product conversion. Literally hundreds of investigators have contributed to what is now regarded as a fairly practical description of the behavior of a fluidized bed;

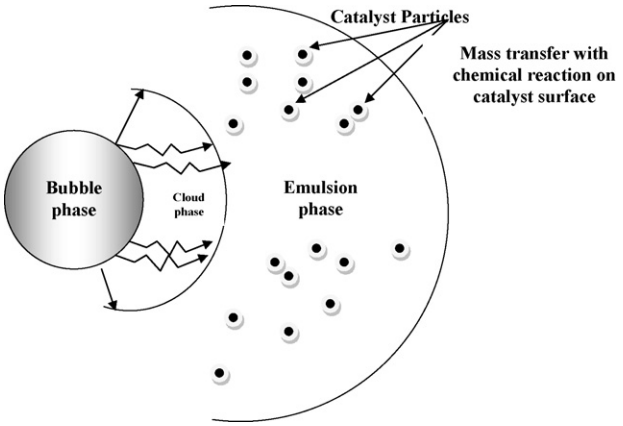

Fig. 1. Steps of the polymerization process.

Table 1a
List of model assumptions

1 The fluidized bed comprises three phases: bubble, cloud, emulsion and solid phases.
2 Polymerization reactions occur in emulsion and solid phases.
3 The emulsion phase is at minimum fluidizing conditions.
4 Gas in excess of that required to maintain the minimum fluidizing condition passes through the bed as the bubble phase.
5 There are negligible radial temperature and concentration gradients in the bed, due to the agitation produced by the up-flowing gas.
6 There is not negligible resistance to mass transfer between emulsion and solid phase.
7 The gas phase is composed of ethylene, 1-butene, 1-hexene, nitrogen and hydrogen.
8 The dynamic of reactions is represented by the rate of reaction at the surface of two kinds of catalysts rigid and porous catalysts.
9 In this model mass transfer of emulsion molecules occurs on the catalyst solid particles and reacts at the surface of catalysts particles (surface reaction) with propagation of polymer particles.

among these is the work of Davidson et al. and Choi and Ray [1], McAuley et al. [2], Hatzantonis et al. [3]. Early investigators saw that the fluidized bed had to be treated as a two-phase system only: an emulsion phase and a bubble phase (often called the *dense* and *lean phases*) without considering the effects of the solid phase. The bubbles contain very small amount of solids [7–10]. Each bubble of gas has a wake which contains a significant amount of solids. As the bubble rises, it pulls up the wake with its solids behind it. The net flow of the solids in the emulsion phase must therefore be downward. The gas within a particular bubble remains largely within that bubble, penetrating only a short distance into the surrounding emulsion phase. The region penetrated by gas from a rising bubble is called the cloud. Emulsions are part of a more general class of two-phase systems of matter called colloids. In the present model, these observations were combined with some improving assumptions to provide a practical, usable model of the fluidized-bed behavior. The model assumptions are listed in Table 1a and the difference between our model and all the well known model is shown in Table 1b.

Table 2
Numerical values of the kinetic rate constants for adsorption, surface and desorption reactions inside the catalyst layers

Rate constant (s^{-1})	Site type	
	1	2
Reactant adsorption (K_A)	0.001	0.001
Activation energy (E) (kcal/mol)	9	9
Surface reaction (K_S)	0.001	0.001
Activation energy (E) (kcal/mol)	9	9
Product desorption (K_D)	0.00047	0.00047
Activation energy (E) (kcal/mol)	9	9
$M_j + s \rightleftarrows M_{j,s}$	Reactant adsorption	
$M_{j,s} \rightarrow P_{n,i,s}$	Surface reaction	
$P_{n,i,s} \rightarrow P_{n,i}, + s$	Product desorption	

2.2. Reaction kinetics

In the present study, a comprehensive mechanism is considered to describe the copolymerization kinetics of ethylene and 1-butane over a Ziegler–Natta catalyst with two different catalyst porosity and rigid catalyst sites based on the kinetic model proposed by McAuley et al. [2]. Rates of formation, initiation, propagation and chain transfer are different for each site type. This mechanism comprises of series and parallel elementary reactions as listed in Table 2. The rate constants used in this study are those given by kinetic and pseudo-kinetic [2] and the activation energies are taken from [9] for porous catalysts the effects of adsorption, desorption and surface reaction are included in the rate of chemical reaction. The reactions are listed in Table 3. Side reactions with poisons are neglected in the present work.

The moment equations are given in Table 4. The method of moments for live and dead moment is applied for the predication of the physicochemical characteristics of the polymer such as molecular weight, polydispersity index and melt flow index.

Table 1b
Differences between the modified model and the other models

No.	Functions	Modified mathematical model	Constant bubble size model	Bubble growth model	Well-mixed model
1	Phases	Bubble, emulsion and cloud	Bubble and emulsion	Bubble and emulsion	Only one phase
2	Mass transfer from bubble to the cloud	Mass transfer from bubble to the cloud without chemical reaction	Not calculated	Not calculated	Not calculated
3	Mass transfer from cloud to the emulsion	Mass transfer from cloud to the emulsion without chemical reaction	Mass transfer from bubble to the emulsion with chemical reaction	Mass transfer from bubble to the emulsion with chemical reaction	One temperature and concentration change represented by one phase only
4	Mass transfer from emulsion to the solid	Mass transfer from emulsion to the solid with a chemical reaction	Not found	Not found	Not found
5	Rate of reaction	Two types of rate of reaction for catalysts porous and rigid.	Activation reaction not depending on the types of catalysts	Activation reaction not depending on the types of catalysts	Activation reaction not depending on the types of catalysts
6	Energy transfer	Solid phase considered	Solid phase ignored	Solid phase ignored	Solid phase ignored

Table 3
Kinetic mechanism of olefin copolymerization for rigid Ziegler–Natta catalyst

Spontaneous activation: $P^0 \xrightarrow{k^n} P_0$
Initiation: $P_0 + M_j \xrightarrow{k_j^i} P_{1,j}, \quad j = 1, 2$
(Formation of $P_{1,i}$: $P_0 + M_i \xrightarrow{k_i^i} P_{1,i}, \quad i = 1, 2$)
Propagation: $P_{n,i} + M_j \xrightarrow{k_{i,j}^P} P_{n+1,j}, \quad i, j = 1, 2, n = 1, 2, \ldots, \infty$
(Consumption of $P_{1,i}$: $P_{1,i} + M_i \xrightarrow{k_{i,j}^P} P_{2,j}, \quad i, j = 1, 2, n = 1, 2, \ldots, \infty$)
(Formation of $P_{n,i}$: $P_{n-1,i'} + M_i \xrightarrow{k_{i',i}^P} P_{n,i}, \quad i', i = 1, 2, n = 1, 2, \ldots, \infty$)
Chain transfer: $P_{n,i} + M_j \xrightarrow{k_{i,j}^f} P_{1,j} + Q_n, \quad i, j = 1, 2, n = 1, 2, \ldots, \infty$
$P_{n,i} + H_2 \xrightarrow{k_i^h} P_0^* + Q_n, \quad i, j = 1, 2, n = 1, 2, \ldots, \infty$
(Formation of $P_{1,i}$: $P_{n,i'} + M_i \xrightarrow{k_{i',i}^f} P_{1,i} + Q_n, \quad i', j = 1, 2, n = 1, 2, \ldots, \infty$)
(Consumption of $P_{1,i}$: $P_{1,i} + M_j \xrightarrow{k_{i,i}^f} P_{1,j} + Q_1, \quad i, j = 1, 2$)
(Consumption of $P_{1,i}$: $P_{1,i} + H_2 \xrightarrow{k_i^h} P_0^* + Q_1, \quad i, j = 1, 2$)

From the kinetic mechanism, the rate expression for the active sites (r_a) for each species can be written as follows:

$$r_a = \text{Active site formation} - \text{Active site consumption}$$

$$= k^n[P^0] - \sum_{j=1}^{2} k_j^i[P_0][M_j] \tag{1}$$

The derivation of the rate expressions based on the kinetic mechanism for rigid catalyst is given in Table 2.

The over all rate expression for live and dead moment is represented in Eqs. (2) and (3) respectively, as seen below.

Rate expressions for live moments is given as;

$$R_{\mu_{n,i}}^k = -r_{P_0} \times P_{n,i} - (r_{H_2} \times P_{n,i}^k) - (r_{P_{n,i}} \times P_{n,i}) + \delta(n)\left(\sum_{j=1}^{n} k^h \mu_0 M_i + k^i M_i\right)(1 - \delta(n))\sum_{j=1}^{n} k_j^P M_i P_{n-1,j} - \sum_{j=1}^{n} k_j^P M_j P_{n,j} \tag{2}$$

where $\delta(n)$ is the Kronecker's delta function (e.g., $\delta(n) = 1$ for $n = 1$ and $\delta(n) = 0$ for $n\delta(n) \neq 1$).

Rate expressions for dead moments is given as;

$$R_{\nu_{n,i}}^k = (k^f[M] + k^h[H_2])\mu_n \tag{3}$$

The dynamic mass balance for the catalyst is given as:

$$\frac{dC_{cat}}{dt} = \frac{F_{cat}}{W_S} - \frac{Q_0 C_{cat}\rho_{cat}}{W_S} \tag{4}$$

Table 4
Moment equations for live and dead polymer

$\frac{\partial \mu_0}{\partial t} = P_{n,0}[-r_{P_0} - r_{P_{n,i}} + M_T \times k_{i,j}^P] + k_i^h \times M_T$
$\frac{\partial \mu_1}{\partial t} = P_{n,1}[-r_{P_0} - r_{P_{n,i}}] + P_{n,0}M_T[k_{i,j}^P + k_{i,i}^P] + k_i^h \times M_T$
$\frac{\partial \mu_2}{\partial t} = P_{n,2}[-r_{P_0} - r_{P_{n,i}}] + P_{n,0}M_T k_{i,j}^P + M_T k_{i,j}^P[P_{n,0} + 2P_{n,1}] + k_i^h \times M_T$
$\frac{\partial \nu_0}{\partial t} = (k^f[M_T] + k^h[H_2])\mu_0$
$\frac{\partial \nu_1}{\partial t} = (k^f[M_T] + k^h[H_2])\mu_1$
$\frac{\partial \nu_2}{\partial t} = (k^f[M_T] + k^h[H_2])\mu_2$

Table 5
Estimation of the reactor model parameters for mathematical model system

$\varepsilon_{mf} = 0.586\Psi^{-0.72}\left(\frac{\mu^2}{\rho_g \eta d_p^3}\right)^{0.029}\left(\frac{\rho_g}{\rho_c}\right)^{0.021}$
$\Psi = 1.6$ for $D_{bed} > 1$ m
$\eta = g(\rho_c - \rho_g)$
$u_{mf} = \frac{(\Psi d_p)^2}{150\mu}\eta\frac{\varepsilon_{mf}^3}{1-\varepsilon_{mf}}$
$d_{bm} = 0.652[A_c(u_0 - u_{mf})]^{0.4}$
$\frac{d_{bm} - d_b}{d_{bm} - d_{b0}} = e^{-0.3h/D_t}$
$u_b = u_0 - u_{mf} + (0.71)(gd_p)^{1/2}$
$K_{bc} = 4.5\left(\frac{u_{mf}}{d_p}\right) + 5.85\left(\frac{D^{1/2}g^{1/4}}{d_p^{5/4}}\right)$
$K_{ce} = 6.77\left(\frac{D_g\varepsilon_{mf}u_b}{d_p^3}\right)^{1/2}$
$H_{bc} = 4.5\left(\frac{u_{mf}\rho_g C_{pg}}{d_b}\right) + 5.85\frac{(k_g\rho_g C_{pg})^{1/2}g^{1/4}}{d_b^{5/4}}$
$H_{ce} = 6.77\frac{(k_g\rho_g C_{pg})^{1/2}(\varepsilon_{mf}u_b)^{1/2}}{(d_b^3)^{1/2}}$
$k_{be} = (1/k_{bc} + 1/k_{ce})^{-1}; \quad H_{be} = (1/H_{bc} + 1/H_{ce})^{-1}$
$MFI = 3.346 \times 10^{17} M_w^{-3.472}$

Similarly, the mass balance for the potential active sites and active sites, are

$$\frac{d[P^0]}{dt} = \frac{F_{cat}P_{in}^0}{W_S} - \frac{Q_0 P^0 \rho_{cat}}{W_S} - r_{P^0} \tag{5}$$

and

$$\frac{d[P_0]}{dt} = \frac{F_{cat}P_0}{W_S} - \frac{Q_0 P_0 \rho_{cat}}{W_S} - r_{P_0} \tag{6}$$

The rate expression for each species of porous catalyst can be written and the rate expression for the active sites r_a can be written as follows:

$$M_j = \left[\frac{m_T - P_{n,i}/K_D}{1 + P_A K_A}\right] P_A K_A \tag{7}$$

From the kinetic mechanism, the rate expression for the active sites r_a can be written as follows:

$$r_a = \text{Active site formation} - \text{Active site consumption}$$

$$= k^n P^0 - \sum_{j=1}^{2} k_j^i P_0 \left[\frac{M_T - P_{n,i}/k_D}{1 + P_A k_A}\right] P_A k_A = k^n P^0 - \sum_{j=1}^{2} k_j^i P_0 M_j \tag{8}$$

The rate of reaction r_a is used in calculations of the emulsion temperature and concentration in Eqs. (13) and (14) respectively.

2.3. Fluidized-bed reactor modeling

The estimation of the reactor model parameters are given in Table 5. From Fig. 1, it can be seen that the polymerization process in the fluidized-bed reactor (FBR) occurs in three basic steps as, follows:

1. Bubble phase to cloud phase (Step 1).
2. Cloud phase to emulsion phase (Step 2).
3. Mass transfer with chemical reaction from emulsion phase to the catalyst phase and propagation in size and molecular weight of the polyethylene particle (Step 3).

The mass and energy balance equations pertinent to each of these steps are described below where the meaning of all symbols can be found in the nomenclature section.

2.3.1. Bubble phase to cloud phase of ethylene (Step 1)

Mass balance;

$$u_b \frac{dC_{Ab}}{dZ} = -K_{bc}(C_{Ab} - C_{Ac}) \quad \text{At } Z = 0,\ C_{Ab} = C_{Ab0} \tag{9}$$

Heat balance;

$$\frac{d}{dZ}[C_{Ab}(T_b - T_{ref})] = \frac{H_{bc}}{u_b C_{pg}}(T_c - T_b) \tag{10}$$

2.3.2. Cloud phase to emulsion phase (Step 2)

Mass balance;

$$u_b \delta \left[\frac{3(u_{mf}/\varepsilon_{mf})}{u_b - (u_{mf}/\varepsilon_{mf})} + \alpha\right] \frac{dC_{Ac}}{dz} = K_{bc}(C_{Ab} - C_{Ac}) - K_{ce}(C_{Ac} - C_{Ae}) \tag{11}$$

Heat balance;

$$z \frac{d}{dZ}[C_{Ac}(T_c - T_{ref})] = \frac{H_{ce}}{u_c C_{pg}}(T_e - T_c) \tag{12}$$

2.3.3. Mass transfer with chemical reaction from emulsion phase to the catalyst phase and propagation in size of the polyethylene particle

Mass balance;

$$A_1 H \varepsilon_{mf} \frac{dC_{me}}{dt} = K_{ce}[C_{Ac} - C_{Ae}]A_1 H \varepsilon_{mf} + G1(C_{AO} - C_{me}) - Q_0 C_{me} \varepsilon_{mf} + r_a W_S \tag{13}$$

Heat balance;

$$A_1 H[(1-\varepsilon_{mf})\rho_s C_{ps} + \varepsilon_{mf} C_{mf} C_{pg}]\frac{dT_e}{dt} + A_1 H(T_e - T_{ref})\varepsilon_{mf} C_{pg} \frac{dC_{me}}{dt} = -GC_{me}C_{pg}(T_e - T_f) + A_B H_{be} \int (T_b - T_e)dz + (-\Delta H_r) r_a - Q_0(\varepsilon_{mf})C_{me}C_{pg}(T_e - T_{fs}) - Q_0 \varepsilon_{mf} C_{me} C_{pg}(T_e - T_f) - \pi D H (1-\delta^*) h_w (T_e - T_w) \tag{14}$$

After mass transfer to the catalysts particles (Step 3), chemical reaction happens on the surface of the catalyst and propagates within the polymer particles. This will cause the polyethylene particles to produce and grow. The particle growth is assumed to be of spherical shape given by;

$$\frac{d(4r^3\pi)}{3dt} = \frac{M_W(\text{catalyst}) \times r_a \times M(\text{mass of catalyst})}{\rho_c}$$
$$\frac{d(r^3)}{dt} = \frac{M_W \times r_a \times M \times 0.75}{\pi \rho_c} \tag{15}$$

The dynamic balances for all other species X^k (e.g., $\mu_0^k, \mu_1^k, \mu_2^k, v_0^k, v_1^k, v_2^k$) can be expressed as:

$$\frac{dX^k}{dt} = R_X^k - \frac{Q_0 X^k \rho_{cat}}{W_S} \tag{16}$$

These leading moments are used in the calculation of average molecular weight M_w and number average molecular weight M_n.

$$W = \frac{\sum_{j=1}^{2} W_j[M_j]}{\sum_{j=1}^{2}[M_j]} \tag{17}$$

$$M_n = W\left(\frac{\mu_1 + v_1}{\mu_0 + v_0}\right) \tag{18}$$

$$M_w = W\left(\frac{\mu_2 + v_2}{\mu_1 + v_1}\right) \tag{19}$$

Table 6
Physical constants and operating parameters for the mathematical model system

$C_{pg} = 1.84 \times 10^3$ J/(kg K)
$C_{ps} = 1.91 \times 10^3$ J/(kg K)
$D = 2.5$ (m)
$D_G = 6.0 \times 10^{-7}$ m^2/s
$E_a = 3.76 \times 10^4$ J/mol
$H = 6$ m
$k_g = 3.2 \times 10^{-2}$ J/(m s K)
$k_{po} = 4.17 \times 10^3$ m^3/(kg cat s)
$(-\Delta H_r) = 3.829 \times 10^6$ J/kg
$u_0 = 0.4$ m/s
$\rho_g = 29$ kg/m^3
$\rho_s = 2.37 \times 10^3$ kg/m^3
$\mu = 1.16 \times 10^{-5}$ kg/(m s)
$C_0 = 20$ kg/m^3
$q_c = 1.39 \times 10^{-4}$ g/s
$T_{ref} = 300$ K
$T_f/T_{ref} = 1.0$
$T_w/T_{ref} = 1.1$
Ethylene concentration = 40%
1–Butene concentration = 17%
Hydrogen concentration = 9%
Inert gas concentration = 34%

where W_j is the ratio of molecular weight of the monomer to that of the co-monomer.

The relation between the melt flow index (MFI) and the molecular weight of polyethylene is given by the following equation:

$$\text{MFI} = 3.346 \times 10^{17} M_w^{-3.472} \ \text{(g/min)} \tag{20}$$

Polydispersity index (PDI) is defined as the ratio of the average molecular weight to the number average molecular weight [11,5,12,8] given as:

$$\text{PDI} = \frac{M_w}{M_n} \tag{21}$$

2.3.4. Estimation of the reactor model parameters

Model parameters include the bubble velocity at which the bubbles move through the column (u_b), minimum fluidized velocity (u_{mf}), minimum fluidizing emissivity (ε_{mf}), reactor shape factor (Ψ), mass transfer driving force (η), particle diameter (d_p), maximum bubble diameter (d_{bm}), melt flow index and mass and heart transfer coefficients. These parameters are calculated using semi-empirical and empirical corrections. Table 5 gives a list of these correlations.

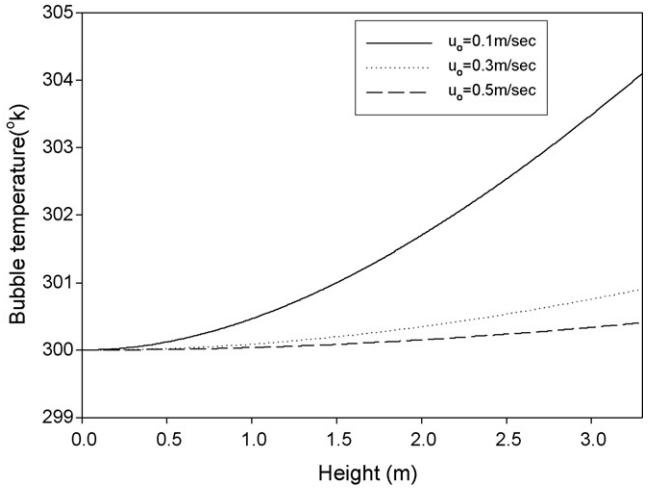

Fig. 2. Effects of superficial velocity on monomer temperature in the bubble phase with variable height.

3. Model solution and analysis

The previously described process model Eqs. (1)–(21) incorporating the parameter values of Table 5 were solved in Matlab using the Differential Algebraic Equation (DAE) solver with the fourth order Runge–Kutta method (Table 6).

The process was simulated for the effects of superficial velocity on monomer temperature in the bubble phase with variable height and effects of superficial velocity and catalyst flow rate in the emulsion phase with variable time on emulsion temperature, emulsion concentration and molecular weight of the phase.

In the following sections the simulation results are described for the different phases of the system.

3.1. Bubble phase

Fig. 2 shows the effect of gas velocity on the monomer temperature in the bubble phase for different superficial gas velocities thorough the reactor height. The temperature profile has an inverse relationship with the increase in superficial gas velocity. However, the rate of change in the temperature is higher at low superficial gas velocity and decreases as the superficial gas velocity value becomes larger. Since the mass and heat transfer coefficient decreases with increase of superficial velocity this will lead to reduction in the concentration and decrease of the bubble temperature with change of column height.

3.2. Emulsion phase

Figs. 3 and 4 show the effect of superficial gas velocity and catalyst flow rate respectively on the temperature, concentration and molecular weight in the emulsion phase with respect to time.

It can be seen that the emulsion temperature, monomer concentration and molecular weight in the emulsion phase depend on the values of superficial gas velocity and catalyst flow rate. The emulsion temperature and molecular weight have an inverse relationship with the increase in superficial gas velocity. The change

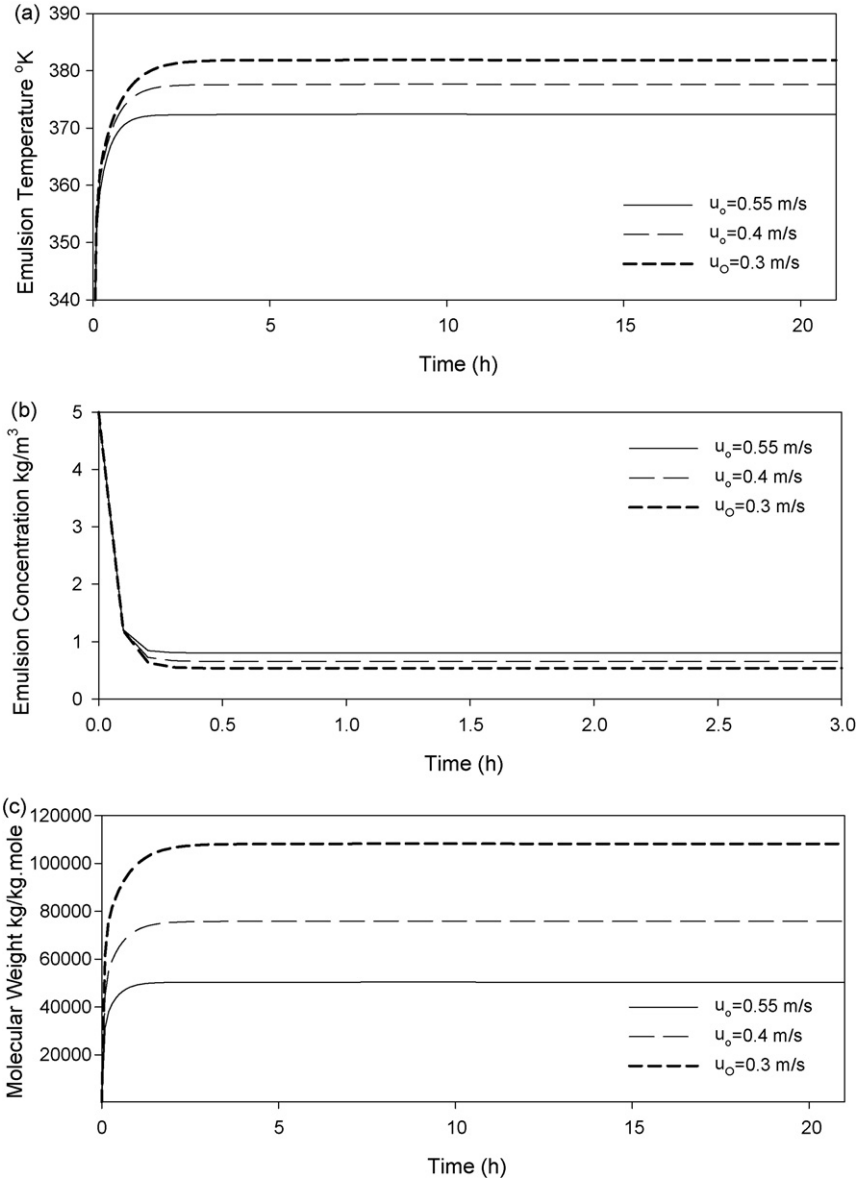

Fig. 3. Effects of superficial velocity in the emulsion phase with variable time for (a) emulsion temperature, (b) emulsion concentration and (c) molecular weight.

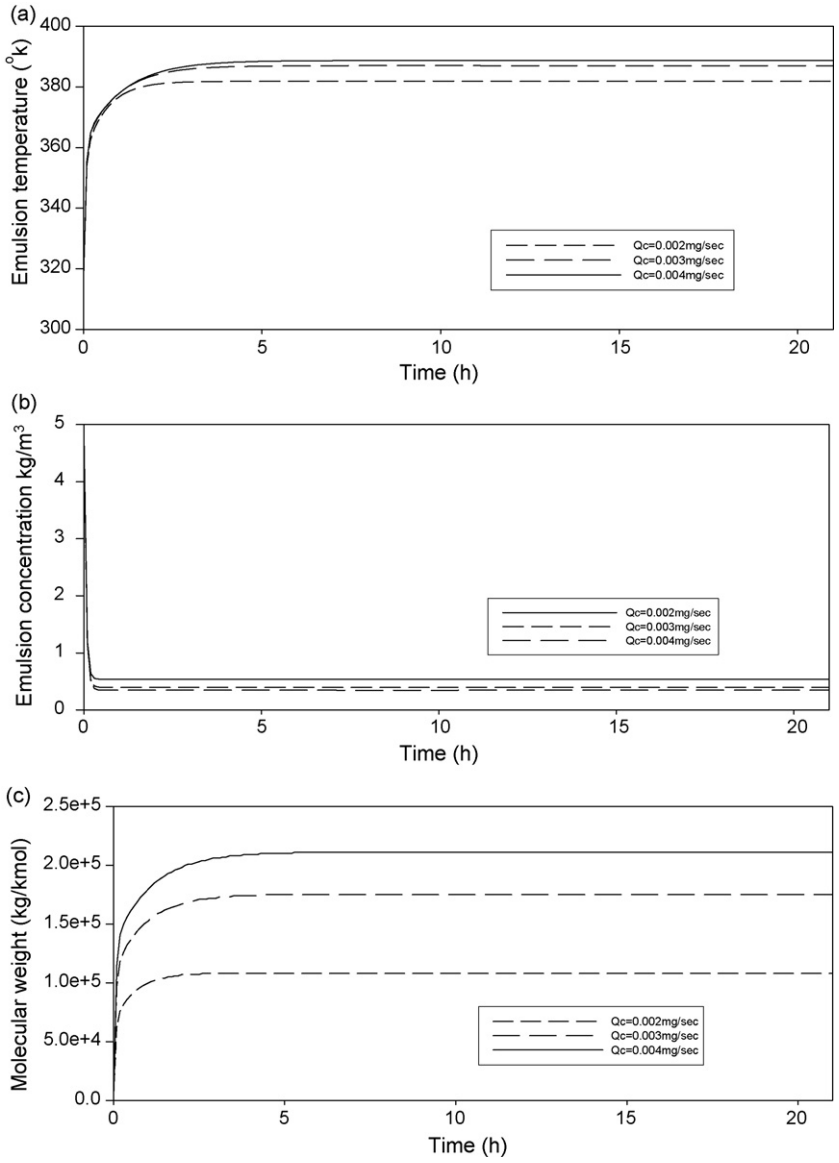

Fig. 4. Effect of variation in catalyst flow rate in the emulsion phase for: (a) emulsion temperature, (b) emulsion concentration and (c) molecular weight with variable time.

in emulsion concentration has an inverse relationship with the increase in superficial gas velocity because the mass and heat transfer coefficient have inverse relationship with increase superficial velocity so, the emulsion concentration reduce that leads to decrease in the rate of reaction, emulsion temperature and molecular weight. The emulsion temperature, molecular weight and emulsion concentration proportionally increases with catalyst flow rate because there is an increase of the rate of reaction that leads to the increase in emulsion temperature and molecular weight. All these behavior are shown in Figs. 3 and 4 respectively.

3.3. Polyethylene particles growth

The types of catalyst used affect the propagation of radius polymer particles due to the adsorption of porous catalyst. This reduced rate of reaction will have bigger effects on the propagation of catalyst compared to the nonporous catalyst. Model predictions of the particles growth for porous and nonporous catalysts are shown in Fig. 5. For emulsion temperature, the effect

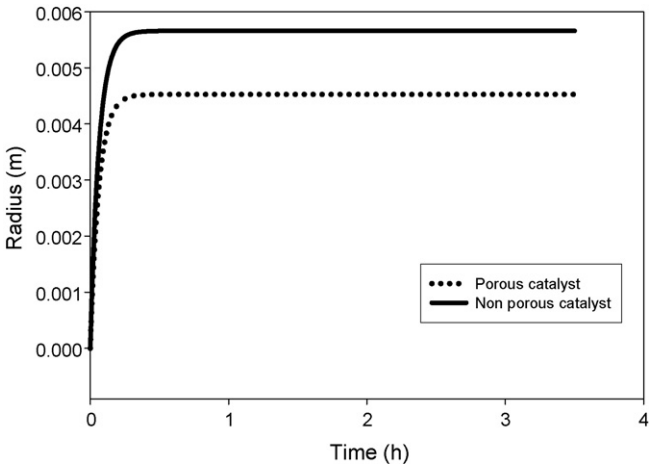

Fig. 5. Effect of catalyst types on particle growth with time for porous and nonporous catalyst cases.

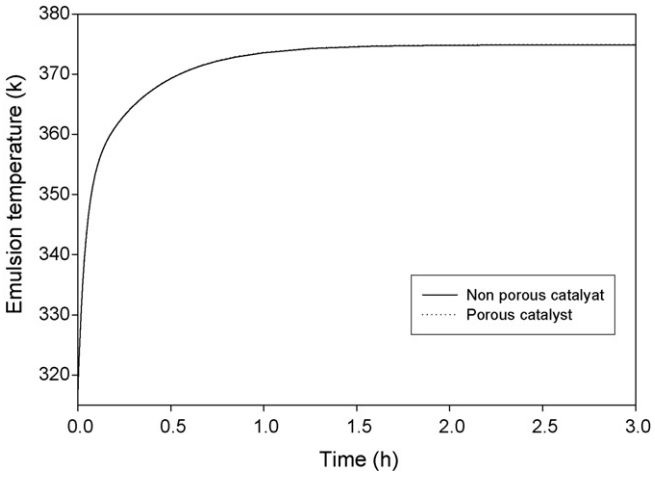

Fig. 6. Effect of catalyst types on emulsion temperature with time for porous and nonporous catalyst cases.

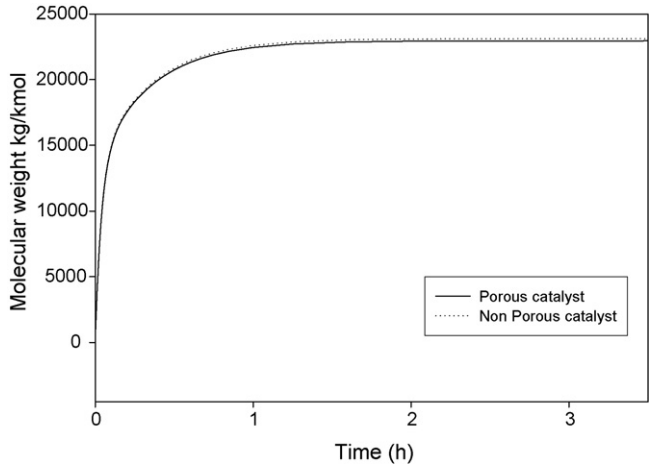

Fig. 7. Evaluation weight average molecular weight during the residence time of polymer for fcat = 0.001 g/s in the reactor for porous and nonporous catalyst.

of catalyst type used is not found to be significant as shown in Fig. 6.

3.4. Number average, weight average molecular weight of polymer, and polydispersity index

Polydispersity index of the polymer is defined as the ratio of weight average molecular weight to the number average molecular weight. Figs. 7–9 show that the type of catalyst have little effect on the number average, weight average molecular weight and the Polydispersity index. These can also be seen in Table 7.

Table 7
Effect of type of catalyst on molecular weight and number average molecular weight calculations at time 3.5 h

	Molecular weight (kg/kmol)	Number average molecular weight (kg/kmol)
Rigid catalyst	106,700	33,406
Porous catalyst	106,300	33,387

fcat = 0.001 g/s.

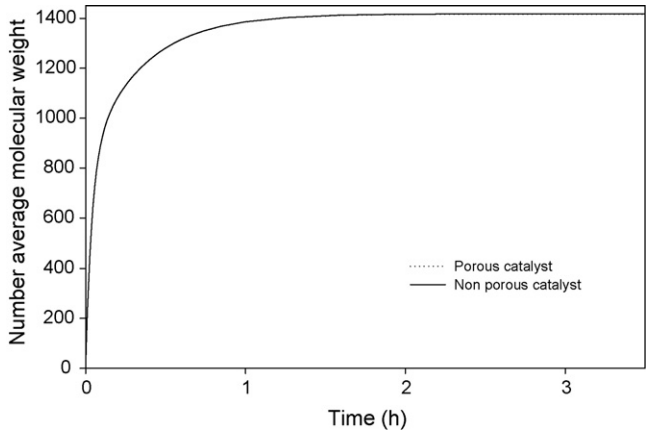

Fig. 8. Evaluation number average molecular weight during the residence time of polymer for fcat = 0.001 g/s in the reactor for porous and not porous catalyst.

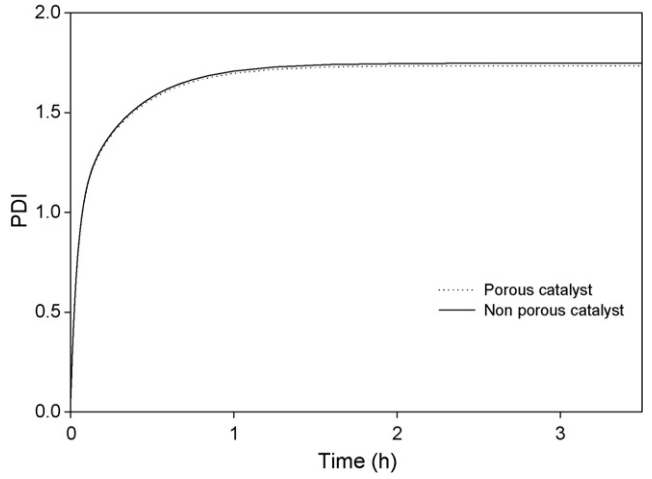

Fig. 9. Evaluation of polydispersity index during the residence time of polymer in the reactor for porous and not porous catalyst.

4. Model validation with previous models and experimental data

Comparison of the three previously available models; the well-mixed model, the constant bubble size model, the bubble growth model and modified model in terms of their dynamic predications is shown in Figs. 10 and 11, and Table 1b. The figure indicates that the predications of the four models are close to each other at the startup conditions of the reactor operation. However this behavior changes as the process dynamics proceeds in time and by the end of the time of reaction, the modified model becomes closer to Hatzantonis (bubble growth model) and Well-mixed model. However the Choi and Ray model (constant bubble size model) has the largest deviation from the modified model.

The close behavior of modified mathematical model to the bubble growth model is mainly due to the fact that the active site reaction happens in the emulsion phase which occupies an area of more than 92% of the total system area. The well-mixed model performance is also, close to the modified mathematical model because in both models the reaction is considered to occur in all the system. The difference between the two models is in the number of phases considered. The constant bubble size model considers two phases but the rate of reaction does not occur in all the system.

In summary the dynamic behavior of the modified model is very close to the bubble growth and well-mixed models in the

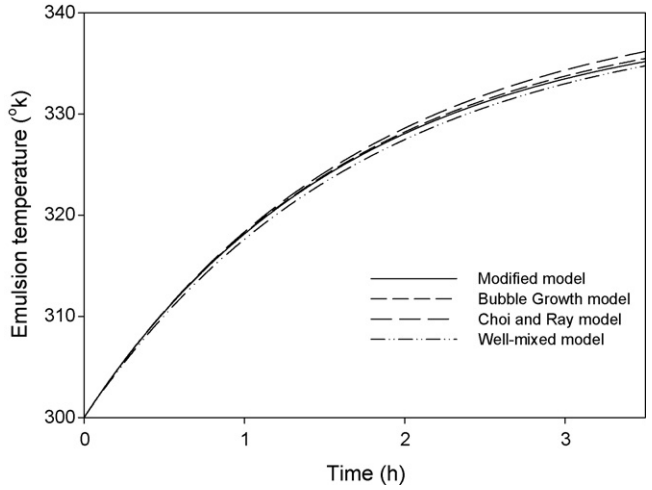

Fig. 10. Comparison behavior of emulsion temperature at $u = 0.3$ m/s between modified model and the other three models

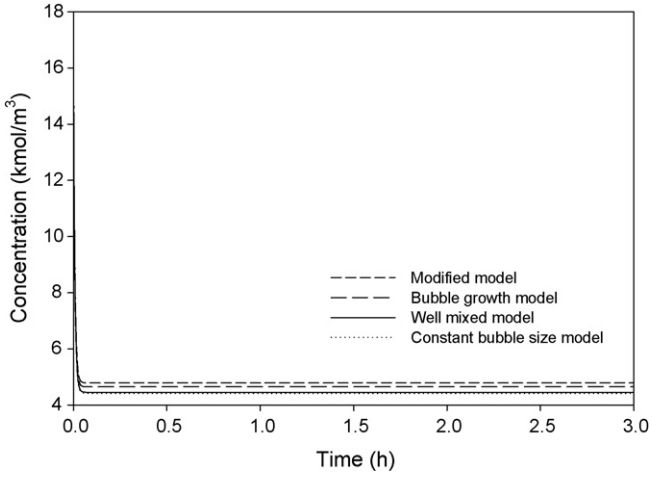

Fig. 11. Comparison behavior of emulsion concentration at $u = 0.3$ m/s between modified model and the other three models

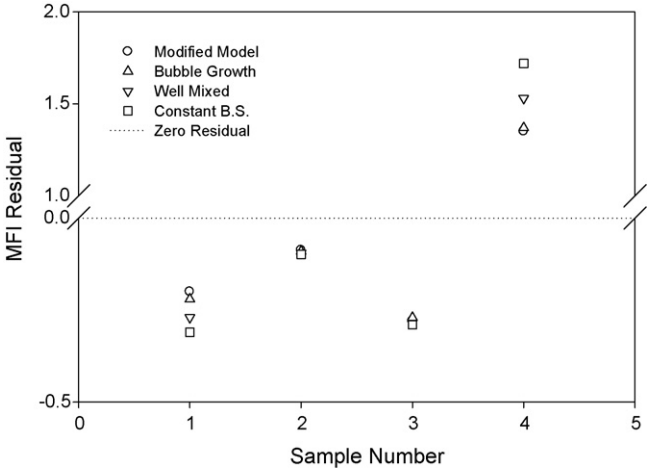

Fig. 12. Actual plant versus model predicted MFI values

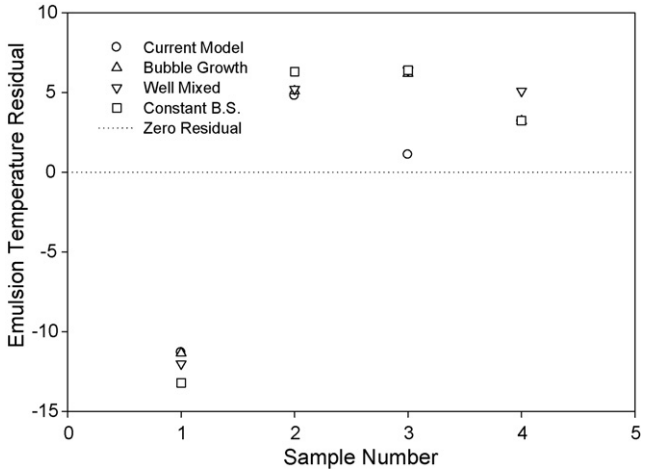

Fig. 13. Actual versus model predicted emulsion temperature

initial stages and starts to differ with change in the time. The accuracy of the steady state behavior of these models can be seen from their comparison with actual plant data [13,14] as shown in Figs. 12 and 13 for the MFI and emulsion temperature respectively. The condition related to the different sample number can be seen in these references [13,14]. Further more the change in butene and hydrogen compositions when one of them increased lead to produce the dead polymer in site active reaction that make the models very close to each other.

5. Conclusion

A modified dynamic three-phase structure model was developed in this work. This model takes into account the presence of particles participating in the reaction with emulsion and catalyst phases which depend on superficial velocity and catalyst feed. In addition, heat and mass transfer between the bubble and the cloud as well as between the cloud and the emulsion phases was included. The solid phase was considered in the mass transfer calculations. Model simulations indicate that it is capable of predicating reactor performance indicators as well as calculating the changes of polymer particles size throughout the transience of the reaction. The model presented in this work was compared with three previously available models and results of the proposed model were compared with experimental data at steady state for MFI and emulsion temperature of the polyethylene production process. From its observed accuracy, we can conveniently use this model as a predictive tool to study the effects of operating, kinetic and hydrodynamics parameters on the reactor performance as well as polymer properties. The comparison results between the modified model and the other three available models gave good indication about the behavior of the present model which is very close to that of the bubble growth model and the well-mixed model in the initial stages but different with change in time. The model developed here will also be used in model-based prediction control to control the reactor which is part of our future work.

References

[1] K.Y. Choi, W.H. Ray, The dynamic behaviour of fluidized bed reactors for solid catalysed gas phase olefin polymerization, Chem. Eng. Sci. 40 (1985) 2261–2279.
[2] K.B. McAuley, J.F. MacGregor, A.E. Hamielec, A kinetic model for industrial gas-phase ethylene copolymerization, AIChE Journal 36 (6) (1990) 837–850.
[3] H. Hatzantonis, H. Yiannoulakis, A. Yiagopoulos, C. Kiparissides, Recent developments in modeling gas-phase catalyst olefin polymerization fluidized bed

reactor: the effect of bubble size variation on the reactor's performance, Chemical Engineering Science 5 (2000) 3237–3259.
[4] C. Chatzidoukas, J.D. Perkins, E.N. Pistikopoulos, C. Kiparissides, Optimal grade transition and selection of closed-loop controllers in a gas-phase olefin polymerization fluidized bed reactor, Chemical Engineering Science 58 (2003) 3643–3658.
[5] R. Sala, F. Valz-Gris, L. Zanderighi, A fluid-dynamic study of a continuous polymerisation reactor, Chemical Engineering Science 29 (11) (1974) 2205–2212.
[6] R.J. Zeman, N.R. Amundson, Continuous polymerization models—part II: batch reactor polymerization, Chemical Engineering Science 20 (7) (1965) 637–664.
[7] Xuejing Zheng, Makarand S. Pimplapure, Günter Weickert, Joachim Loos, Study the porosity effects of Ziegler–Natta catalyst on polymerization system, European Polymer Journal 68 (2006) 680–688.
[8] Victor M. Zavala, Antonio Flores-Tlacuahuac, Eduardo Vivaldo-Lima, Dynamic optimization of a semi-batch reactor for polyurethane production, Chemical Engineering Science 60 (11) (2005) 3061–3079.
[9] M. Mourad, M. Hémati, C. LaguérieMing, Drying of maize in a fluidized bed: II: a kinetic model of drying, The Chemical Engineering Journal and the Biochemical Engineering Journal 60 (1–3, 12) (1995) 39–47.
[10] Mariano Asteasuain, Alberto Bandoni, Claudia Sarmoria, Adriana Brandolin, Simultaneous process and control system design for grade transition in styrene polymerization, Chemical Engineering Science 61 (10) (2006) 3362–3378.
[11] Roberto Lemoine-Nava, Antonio Flores-Tlacuahuac, Enrique Saldívar-Guerra, Non-linear bifurcation analysis of the living nitroxide-mediated radical polymerization of styrene in a CSTR, Chemical Engineering Science 61 (2) (2006) 370–387.
[12] R.J. Zeman, N.R. Amundson, Continuous polymerization models—part II: Batch reactor polymerization' Chemical, Engineering Science 20 (7) (1965) 637–664.
[13] Mahmood Alizadeh, Navid Mostoufi, Saeed Pourmahdian, Rahmat Sotudeh-Gharebagh, Modeling of fluidized bed reactor of ethylene polymerization, Chemical Engineering Journal 97 (2004) 27–35.
[14] Ali Kiashemshaki, Navid Mostoufi, Saeed Pourmahdian, Rahmat Sotudeh-Gharebagh, Two phase Modeling of a gas phase polyethylene fluidized bed reactor, Chemical Engineering Science 61 (2006) 3997–4006.